

Oscillatory Motion of Rising Bubbles in Wormlike Micellar Fluids with Different Microstructures

Nestor Z. Handzy and Andrew Belmonte

*The W. G. Pritchard Laboratories, Department of Mathematics,
Penn State University, University Park, PA 16802*

(Dated: October 15, 2003; submitted January 10, 2003)

Previous observations of the nontransient oscillations of rising bubbles and falling spheres in wormlike micellar fluids were limited to a single surfactant system. We present an extensive survey of rising bubbles in another system, an aqueous solution of cetylpyridinium chloride and sodium salicylate, with and without NaCl, across a range of concentrations and temperatures. Two different types of oscillation are seen in different concentration ranges, each with its own temperature dependence. Rheological data allows for the identification of these different hydrodynamic states with different fluid microstructures.

PACS numbers: 47.50.+d, 83.50.Jf, 83.60.Wc

Fluids are often broadly categorized as either Newtonian or non-Newtonian, according to whether the Navier-Stokes equation does or does not accurately describe the fluid's motion. Newtonian fluids consist of molecules small enough to be approximated by point masses (such as air and water), while non-Newtonian consist of larger structures (such as polymers). This increased size affords greater degrees of freedom which leads to macroscopic viscoelasticity [1]. Fluids consisting of self-assembling cylindrical (or wormlike) micelles resemble polymeric fluids on the microscopic scale, with the added feature that their length distribution is determined by aggregation kinetics; micelles continually break and reform [2, 3, 4]. The molecular level physics is clearly more complicated for such fluids, and one can reasonably expect this will introduce a new set of flow properties to the class of non-Newtonian fluids.

Several novel results have been reported in both viscometric flows [5, 6, 7, 8, 9] and hydrodynamic (non-viscometric) flows [10, 11, 12] of various wormlike micellar fluids. Among these, a falling pendant drop at the bottom of a thin filament has been observed to slow to a complete stop before the filament suddenly ruptures [10]; this rupture has been confirmed in other configurations [13]. Also, rising air bubbles and falling solid spheres have been observed to oscillate without reaching a terminal velocity [11, 12]. While in polymer solutions a rising bubble displays a sharp non-axisymmetric cusp, which remains unchanged during a steady rise [1, 14], in wormlike micellar fluids the cusp periodically extends to a sharp point, then retracts to a blunt edge (see Fig.1). It is likely that these new dynamics are a manifestation of the reversible scission reactions of the micelles, though the precise mechanism may be quite complicated. Another type of fluid is known to include scission-like reactions at its microscale - associating polymer solutions - and falling sphere oscillations are reported in that system as well [15, 16].

In this Letter we report a detailed survey of the oscillatory motion of rising bubbles in a wormlike micellar fluid. To study the role of the aggregation kinetics of

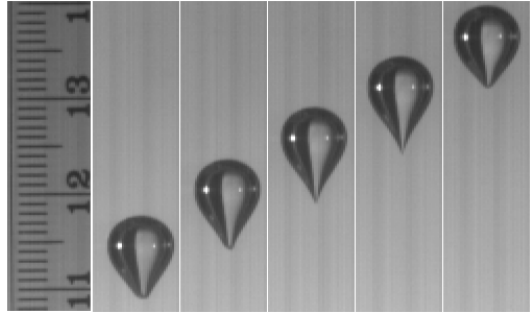


FIG. 1: Cusp shape change of an oscillating bubble rising through a 15mM CPCl/NaSal (weight fraction $\varphi = 0.5\%$) solution at $T = 37.5^\circ\text{C}$. The scale at left is marked in centimeters. Interval between pictures: 0.05 s.

the micelles, both concentration and fluid temperature were varied over a wide range, unlike previous studies [11, 12]. As these parameters change, different micellar architectures are possible - from short linear or branched micelles to crosslinked networks [17, 18, 19]. Four different dynamics were seen: Newtonian behavior at high temperatures, standard polymeric behavior, and two distinct oscillating responses occurring in different concentration ranges (Fig.2). We performed steady rheology experiments to identify the fluid microstate, and found that transitions in the equilibrium structure match transitions in bubble dynamics. Critical temperature bounds were also found, which can be interpreted as a minimum length of micelle required for oscillations to occur, so that for certain concentrations the fluid may be tuned with temperature to make bubbles either oscillate, rise with a stable cusp, or rise as bubbles in a Newtonian fluid.

Non-transient oscillating bubbles were first observed in aqueous solutions of cetyltrimethylammonium bromide (CTAB) and sodium salicylate (NaSal) [11]; here we use another familiar system, cetylpyridinium chloride (CPCl) and NaSal, with the fixed ratio $[\text{NaSal}]/[\text{CPCl}] = 1$ (except for the NaCl experiments described below). Our

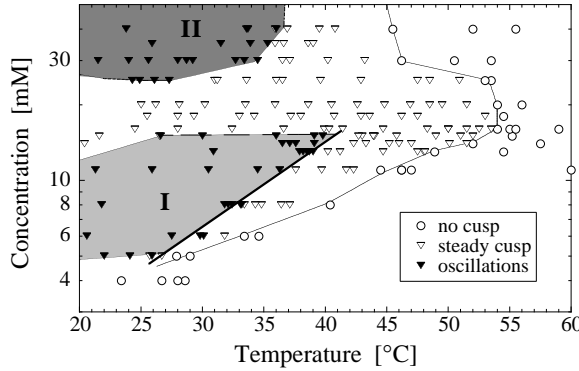


FIG. 2: Temperature and concentration phase diagram for the dynamics of rising bubbles in equimolar CPCl/NaSal, showing two distinct regions of oscillating behavior (shaded) labelled as I and II. The thick sloped line marking the temperature boundary for type I oscillations is an isoline of Eqn. 1.

choice for this ratio gives a solution of flexible cylindrical micelles analogous to polymer chains [5]. All experimental results are for a single rising bubble, with volumes ranging from 14 mm^3 to 110 mm^3 . The bubble is injected into the fluid at the bottom of a temperature controlled plastic cylinder (31 cm height, 5 cm diameter) using a syringe with a long stainless steel tube (inner diameter of either 1.0 mm or 1.5 mm). The ratio of the horizontal diameter of the bubble d to the cylinder diameter D is $d/D \leq 0.14$, and we have also checked that bubbles oscillate for $d/D \simeq 0.02$. Typical sizes of the Reynolds number (inertia) are $Re \simeq 10^{-2} - 5$, while the Deborah number (elasticity) ranged from $De \simeq 1 - 500$, similar to values seen for oscillating bubbles and spheres in CTAB/NaSal [11, 12]. Rheological data were taken with a Rheometrics RFS-III controlled rate of strain rheometer with circulating fluid temperature bath, using a stainless steel Couette geometry. Video images were made with a Kodak high speed CCD camera.

We have studied concentrations from 4 to 40 mM (weight fractions $0.13\% \leq \varphi \leq 1.3\%$). From 5 to 15 mM, bubbles have a cusp which oscillates in length and changes shape (Fig.1). While rising, the cusp lengthens (frames 1-4 in Fig.1) during which the velocity as measured at the top of the bubble is nearly constant. At the apex of the extension, the tail abruptly retracts and the bubble jumps upward (frames 4-5). After this it slows to a nearly constant velocity until the cycle repeats. Typically, bubbles begin to oscillate within 10 seconds of their formation, with a similar time between jumps. These clearly visible oscillations, which we call type I, are apparently not a transient effect; we have observed their persistence for rise distances over one meter, during which there were more than 30 oscillations in $\sim 35 \text{ s}$ (for 8 mM CPCl/NaSal), and velocities more than doubled during a jump. This is the typical type I behavior in the temperature ranges shown in Fig.2, consistent

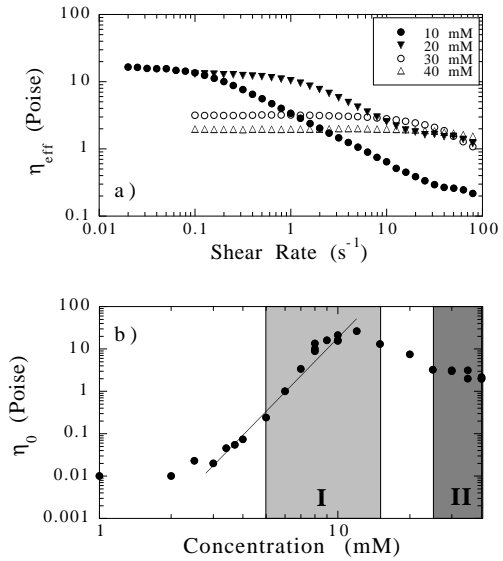


FIG. 3: Rheology of equimolar CPCl/NaSal at 30°C : a) effective viscosity versus shear rate for 10, 20, 30, and 40 mM; b) zero shear viscosity, η_0 as a function of concentration. The shaded regions mark the concentration ranges of bubble oscillations, and the sloped line starting at 3 mM corresponds to $\eta_0 \sim \varphi^{5.8}$.

with the oscillations observed in CTAB/NaSal [11].

Above a critical temperature in the type I range (Fig.2), bubbles have a sharp cusp which does not change in length (“steady cusp” in Fig.2) and velocities smoothly reach a steady state; the oscillatory instability vanishes. By 60°C , the solutions appear Newtonian (“no cusp” in Fig.2): large enough bubbles are ellipsoidal and undergo the well-known side-to-side oscillations [20]. In this temperature range, the micelles must be predominantly spherical or short rigid rods [21].

Upon increasing the concentration from 15 mM to 16 mM ($\varphi = 0.5\%$ to 0.53%), *all oscillations cease*. Bubbles rise steadily with a stable cusp for concentrations up to 20 mM; there are no temperatures at which oscillations occur (Fig.2). It is striking that a rising bubble would be so affected by so slight a concentration change. Note the transition temperature from polymeric to Newtonian behavior reaches a maximum at this concentration (Fig.2).

More surprising is the re-emergence of oscillations for concentrations from 25 mM to 40 mM ($0.8\% \leq \varphi \leq 1.3\%$). Yet here the oscillations, which we call type II, are visibly different from type I oscillations; the shape change involves the entire bubble, whereas in type I it seems restricted to the tail. A type II oscillation begins with a constriction in width near the top, while the whole bubble lengthens. This constriction then travels downward, as if the bubble were squeezing through a hoop. Defining w_{max} to be the maximum (relaxed) width (at

its waist), w_{min} to be its most constricted width, and $\Delta w = w_{max} - w_{min}$, we found $\Delta w/w_{max} = 0.13$ in type II fluids and 0.04 in type I. Length extensions, however, were $\Delta l/l_{min} = 0.25$ in type II and 0.27 in type I; for bubbles rising in CTAB/NaSal, $\Delta l/l_{min} = 0.26$ [11]. This previous study revealed only one type of oscillation, which from the shape dynamics we identify as type I [11].

Although wormlike micelles are comprised of surfactants, it is unlikely that surface tension plays a role in the bubble oscillations, since falling rigid spheres also oscillate [12]. Furthermore, our observation of two oscillation types suggests that the viscoelastic character of the bulk fluid is changing with concentration. We address this with rheology measurements, controlling the shear strain rate $\dot{\gamma}$ and recording the effective viscosity, $\eta_{eff} = \sigma_{xy}/\dot{\gamma}$, where σ_{xy} is the steady shear stress. Transient tests were also performed to ensure that steady state was achieved. Shown in Fig.3a is η_{eff} vs. $\dot{\gamma}$ at 30°C, for fluids in the oscillating and non-oscillating concentration ranges. Most fluids are shear thinning - η_{eff} decreases at high enough $\dot{\gamma}$ - however fluids below 5 mM shear thicken (η_{eff} increases above η_0), typically requiring ~ 100 seconds to reach steady state [9]. Bubbles tested in fluids below 5 mM showed no oscillations or steady cusps. While there is a noticeable difference in the rheology upon increasing from 20 to 30 mM, 30 and 40 mM (type II region) are strikingly similar; they also have a constant viscosity over a broader $\dot{\gamma}$ range than the other fluids. More interestingly, the zero shear viscosity η_0 (defined as the plateau value at low $\dot{\gamma}$) decreases with concentration.

A more complete study of the dependence of η_0 on φ indicates transitions in fluid microstructure (Fig.3b). The transition at low concentration to rapid η_0 growth marks the overlap concentration $\varphi^* \simeq 3$ mM, below which is the dilute regime. Above φ^* is the semi-dilute state, in which micelles exist as individual entangled worms [22]. Here $\eta_0 \sim \varphi^{5.8}$, close to the value 5.4 associated with stress relaxation by reptation [18, 23]. The semi-dilute regime ends near $\varphi \simeq 12 - 15$ mM, followed by an extraordinary decrease of η_0 with concentration, continuing to $\varphi \simeq 30$ mM, after which η_0 varies weakly.

The dramatic change in the concentration dependence of η_0 indicates a transition in the equilibrium fluid structure, coinciding with the loss of type I oscillations. It may be that the entangled micelles in the semi-dilute range have begun to fuse at entanglement points, forming a crosslinked network [18, 23, 24, 25]. The junction nodes are free to slide along the micelles in such a formation, which would account for the decrease in viscosity [18]. If the ratio of crosslinks to entanglement points grows as η_0 decreases, then the new state would be fully formed where η_0 stabilizes near ~ 30 mM (1%), the start of type II oscillations. Note that a crosslinked network state has also been proposed for CTAB/NaSal at $\varphi \simeq 1\%$ [26].

Transitions in micellar morphology would naturally lead to transitions in mechanisms for stress relaxation, which should be observable in the stress field around the rising bubble. These transitions are made evident with

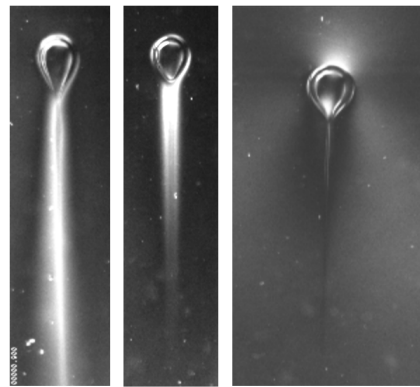


FIG. 4: Birefringent images of the wake behind a bubble rising in CPCl/NaSal at $T = 24^\circ\text{C}$: a) 10 mM ; b) 20 mM ; c) 35 mM. Each image is 6.5 cm high. Reynolds and Deborah numbers for each image are: a) $Re \simeq 4.72$, $De \simeq 250$; b) $Re \simeq 0.02$, $De \simeq 6$; c) $Re \simeq 1.1$, $De \simeq 1.8$.

birefringent visualization, shown in Fig.4 for the three concentration regimes. Optical birefringence is a well-known technique for visualizing stress in non-Newtonian fluids [27], especially effective for wormlike micellar fluids [28]. Fig.4a (10 mM) shows the localization of stress in the wake of a type I oscillating bubble. This birefringent tail mirrors the dynamics of the bubble's cusp (Fig.1), and when it retracts, the birefringent tail suddenly disperses to the sides. The flow in the bubble wake is nearly in uniaxial extension [29], and the birefringent tail suggests a strong relation to a thin filament whose rupture [10] may be related to the mechanism for oscillation. At 20 mM a shorter tail is seen (Fig.4b), whose length remains constant (like the bubble tail). Fig.4c corresponds to type II oscillations (35 mM), in which three equally spaced birefringent bands indicate a broader distribution of stress. This pattern is essentially unaltered during an oscillation. Note that De decreases from type I to type II, with an intermediate value for non-oscillating bubbles (Fig.4 caption), contradicting the implicit critical De condition for oscillations in [12].

The length distribution of the individual worms in the type I region (semi-dilute) should depend on temperature and concentration. In equilibrium, the average length of a wormlike micelle L_0 can be described with the mean field approximation [2, 3, 21]:

$$L_0(\phi, T) \sim \sqrt{\phi} e^{E/2kT} \quad (1)$$

where ϕ is the total amphiphile concentration, k is Boltzmann's constant, T is temperature, and E is the scission energy required to break one wormlike micelle into two. Estimates based on light scattering measurements for E are on the order of $10kT$ [2, 17, 30] - much lower than the covalent bonds of polymers, yet large enough for some micelles to reach appreciable lengths against thermal fluctuations [2]. The flow near the bubble may increase the equilibrium length, and there is evidence

that shear-induced structures (SIS) much larger than individual micelles form in such flow in both CTAB/NaSal [9, 31, 32] and CPCl/NaSal [33, 34]. We assume simply that for the type I region, L_0 is the relevant quantity determining if the bubble will oscillate. Specifically, we attribute the oscillations to a breaking instability of the elongated micelles or SIS in the wake, occurring only if L_0 exceeds some critical value. Using Eqn.1, the solid line in Fig.2 corresponds to a scission energy of $E = 1.01 \times 10^{-19}$ Joules, about $24kT$.

Type II oscillations have a much simpler dependence on temperature; they occur only for $T \lesssim T_c = 36^\circ\text{C}$ (Fig.2). If crosslinks have indeed formed for $T < T_c$, then the mean field length is no longer an appropriate quantity. The transition temperature T_c suggests a critical energy condition ($E_c \simeq 4.3 \times 10^{-21}$ Joules), which may correspond to the energy difference between junctions and endcaps. Thus for $T > T_c$, endcaps would dominate and the fluid is comprised of individual micelles which can entangle like polymers. This possible explanation is consistent with both the rheology and the rising bubble dynamics.

The two different oscillations we have observed appear linked to two different microstructures. We extended our study to include the well characterized ternary system CPCl-NaSal diluted in concentrated NaCl, with a ratio [NaSal]/[CPCl] = 0.5 [8, 22, 35]. We tested several concentrations [36] of these fluids for jumping bubbles in our apparatus, at $T = 30^\circ\text{C}$, a temperature central to both type I and II oscillations (Fig.2). We observed no

oscillations or any behavior different from steadily rising bubbles in conventional polymeric fluids [14]. This classic ternary system is known to consist of entangled wormlike micelles, which when taken with the observed scaling $\eta_0 \sim \varphi^{3.3}$, indicates that micellar breaking occurs on a shorter timescale than reptation [2, 22]; in contrast for our fluids $\eta_0 \sim \varphi^{5.8}$. Evidently, the oscillatory motion of rising bubbles is not a characteristic of fluids in this “fast-breaking” limit [2, 37], and we conclude that type I oscillations are in the “slow-breaking” limit.

Our study of rising bubbles in various wormlike micellar fluids indicates that while scission reactions may be necessary for oscillations, there are other conditions. The discovery of a second type of oscillation provides another example of how microscale dynamics and architecture (entangled vs. crosslinked) interact to produce macroscopic instabilities. It now seems that wormlike micellar fluids are the most generic complex fluids as far as rising bubbles are concerned, since all known material-dependent dynamics can occur at different temperatures or concentrations. More surprisingly, the rise of an air bubble has been shown to be extraordinarily sensitive to fluid microstructure.

We thank A. Jayaraman, J. T. Jacobsen, P. Olmsted, T. Podgorski, and L. M. Walker for valuable discussions, R. Geist, D. M. Henderson, and M. C. Sostarecz for experimental assistance, and the referees for constructive comments. AB acknowledges support from the A. P. Sloan Foundation and the National Science Foundation (CAREER Award DMR-0094167).

[1] R. Bird, R. Armstrong, & O. Hassager, *Dynamics of Polymeric Liquids*, 2nd ed., Wiley and Sons, New York (1987).

[2] M. Cates & S. Candau, *J. Phys.: Condens. Matter* **2**, 6869 (1990).

[3] J. Israelachvili, *Intermolecular and Surface Forces*, 2nd edition, (Academic Press, 1991).

[4] *Micelles, Membranes, Microemulsions, and Monolayers*, W. Gelbart, et al., editors, (Springer, 1994).

[5] H. Rehage & H. Hoffmann, *J. Phys. Chem.* **92**, 4712 (1988).

[6] T. Shikata & H. Hirata, *J. Non-Newtonian Fluid Mech.* **28**, 171 (1988).

[7] C. Grand, J. Arrault, & M. Cates, *J. de Physique II* **7**, 1071 (1997).

[8] S. Lerouge, J-P. Decruppe, J-F. Berret, *Langmuir* **16**, 6464 (2000).

[9] C. Liu & D. Pine, *Phys. Rev. Lett.* **77**, 2121 (1996).

[10] L. Smolka & A. Belmonte, *J. Non-Newtonian Fluid Mech.* **115**, 1 (2003).

[11] A. Belmonte, *Rheol. Acta* **39**, 554 (2000).

[12] A. Jayaraman & A. Belmonte, *Phys. Rev. E* **67**, 65301 (2003).

[13] J. Rothstein, *J. Rheol.* **47**, 1227 (2003).

[14] Y. Liu, T. Liao, & D. Joseph, *J. Fluid Mech.* **304**, 321 (1995).

[15] A. Mollinger, E. Cornelissen, & B. van den Brule, *J. Non-Newtonian Fluid Mech.* **86**, 389 (1999).

[16] P. Weidman, B. Roberts, & S. Eisen, *Progress in Nonlinear Science, Proceedings III*, V.D. Shalfeev ed., (Nizhny Novgorod, 2002), 103.

[17] M. In, G. Warr, & R. Zana, *Phys. Rev. Lett.* **83**, 2278 (1999).

[18] J. Appell, G. Porte, A. Khatory, F. Kern, & S. Candau, *J. de Physique II* **2**, 1045 (1992).

[19] V. Schmitt, F. Lequeux, A. Pousse, & D. Roux, *Langmuir* **10**, 955 (1994).

[20] R. Hartunian & W. Sears, *J. Fluid Mech.* **3**, 27 (1957).

[21] A. Ben-Shaul & W. Gelbart, in [4].

[22] J.-F. Berret, J. Appell, & G. Porte, *Langmuir* **9**, 2851 (1993).

[23] S. Candau, A. Khatory, F. Lequeux, & F. Kern, *J. de Physique IV* **3**, 197 (1993).

[24] T. Drye & M. Cates, *J. Phys. Chem.* **96**, 1367 (1992).

[25] P. Pincus, *Science* **290**, 1307 (2000).

[26] F. Lequeux & S. Candau, in *Theoretical Challenges in the Dynamics of Complex Fluids*, T. McLeish, ed., (Kluwer, 1997).

[27] G. Fuller, *Ann. Rev. Fluid Mech.* **22**, 387 (1990).

[28] Y. Hu, S. Wang, & A. Jamieson, *J. Rheol.* **37**, 531 (1993).

[29] O. Harlen, J. Rallison, & M. Chilcott, *J. Non-Newtonian Fluid Mech.* **34**, 319 (1990).

[30] S. Kwon & M. Kim, *Phys. Rev. Lett.* **89**, 258302 (2002).

[31] P. Boltenhagen, Y. Hu, E. Matthyss, & D. Pine, *Europhys.*

Lett. **38**, 389 (1999).

[32] S. Keller, P. Boltenhagen, D. Pine, & J. Zasadzinski, *Phys. Rev. Lett.* **80**, 2725 (1998).

[33] E. Wheeler, P. Fischer, & G. Fuller, *J. Non-Newtonian Fluid Mech.* **75**, 193 (1998).

[34] P. Fischer, *Rheol. Acta* **39**, 234 (2000).

[35] J.-F. Berret, D. C. Roux, & G. Porte, *J. de Physique II* **4**, 1261 (1994).

[36] Concentrations tested were: $[CPCl] = 30, 40, 50, 60, 70$, and 80 mM , in the system $[NaSal]/[CPCl] = 0.5$ with 500 mM NaCl .

[37] J.-F. Berret, *Langmuir* **13**, 2227 (1997).